

UNCLASSIFIED

AD NUMBER	
AD025266	
CLASSIFICATION CHANGES	
TO:	unclassified
FROM:	confidential
LIMITATION CHANGES	
TO: Approved for public release; distribution is unlimited.	
FROM: Distribution authorized to U.S. Gov't. agencies and their contractors; Administrative/Operational Use; NOV 1953. Other requests shall be referred to Office of Naval research, Arlington, VA.	
AUTHORITY	
ONR ltr, 22 Jun 1955; ONR ltr, 26 Oct 1972	

THIS PAGE IS UNCLASSIFIED

AD No. 25 266

ASTIA FILE COPY

CONFIDENTIAL

MODEL SIMULATION OF TWIN-ROTOR HELICOPTER

DYNAMIC STABILITY AND CONTROL

PHASE I

THEORETICAL ANALYSIS AND MODEL DESIGN

Aeronautical Engineering Laboratory

Report No. 242

November, 1953



PRINCETON UNIVERSITY

DEPARTMENT OF AERONAUTICAL ENGINEERING

CONFIDENTIAL

54A A-3167

DEPARTMENT OF THE NAVY
OFFICE OF NAVAL RESEARCH
Contract N6 onr-27015

CONFIDENTIAL

MODEL SIMULATION OF TWIN-ROTOR HELICOPTER

DYNAMIC STABILITY AND CONTROL

PHASE I

THEORETICAL ANALYSIS AND MODEL DESIGN

Aeronautical Engineering Laboratory

Report No. 242

November, 1953

Prepared by: David F. Gebhard
DAVID F. GEBHARD

Approved by: Leonard Goland
LEONARD GOLAND

A. A. Nikolsky
A. A. NIKOLSKY

CONFIDENTIAL

CH 40-2117

TABLE OF CONTENTS

	Page
1. Summary.	4
2. Introduction.	5
3. List of Symbols.	6
4. Discussion of Simulation Theory.	7
5. Description of Model.	8
6. Theoretical Prediction of Results.	12
7. Proposed Instrumentation and Test Procedure.	16
8. Conclusions.	18
9. References.	19
10. Tables.	20
11. Figures.	23

CONFIDENTIAL

List of Figures

	Page
1. Complete HUP Model Helicopter.	23
2. HUP Model Helicopter Rotor Head.	24
3. HUP Model Helicopter Transmission.	25
4. HUP Model Helicopter Test Blade.	26
5. Completed HUP Model Helicopter Test Blade and Blade Blank.	27
6. Effect of $\frac{1^2 T_E}{2}$ and H_X on Fuselage Oscillation Damping Exponent.	28
7. Effect of $\frac{1^2 T_E}{2}$ and H_X on Fuselage Oscillation Period.	29
8. Effect of $\frac{1^2 T_E}{2}$ and H_X on Fuselage Pitch Response to a Sudden 1.0 Degree Cyclic Pitch Displacement.	30
9. Effect of $\frac{1^2 T_E}{2}$ and K on Fuselage Oscillation Damping Exponent.	31
10. Effect of $\frac{1^2 T_E}{2}$ and K on Fuselage Translational Response to a Sudden 1.0 Degree Cyclic Pitch Displacement.	32
11. Model Power Required vs. Lifted Weight at Various Rotor Speeds.	33

1. Summary

A preliminary design for a six foot diameter twin-rotor helicopter model of the tandem configuration is presented. The purpose of the model is to determine experimentally the longitudinal hovering stability and control characteristics of this helicopter type and to investigate means for improving its handling qualities. The direct model simulation of a full scale helicopter is attempted, the Piasecki HUP being the prototype in this case.

The theoretical stability and control characteristics of the model are presented, and a test procedure based on these results is outlined. The theoretical parameters for an autopilot which will produce excellent hovering handling qualities are also included.

2. Introduction

As a continuation of the helicopter model research carried on at Princeton (References 1, 2, 4, and 6) a twin-rotor helicopter research program has been undertaken. The objectives of this program are briefly as follows:

1. The theoretical analysis of tandem rotor helicopter longitudinal stability and control near hovering flight.
2. The investigation of means for improving the handling qualities of this type of helicopter.
3. The design and test of a model helicopter which can be used to check the validity of the analysis. An effort will be made to simulate the Piasecki HUP helicopter, and the model and supporting members will be designed so that both tandem and side by side rotor configurations with various degrees of overlap can be obtained. The model will utilize the test facility described in Reference 1.

This report covers the first phase of the program; i.e., the design of the model and the preliminary theoretical analysis of the model dynamics. In subsequent phases the model will be built and flown.

3. List of Symbols

- λ = basic scale factor, given linear dimension of full scale helicopter/
corresponding dimension of model.
- l = distance between rotors, ft.
- \dot{T}_z = rate of change of rotor thrust with rotor vertical velocity, lbs.-sec./
ft.
- $\frac{\dot{T}_z}{2}$ = pitch damping moment due to rate of change of rotor thrust with rotor
vertical velocity, ft. lbs.-sec./rad. This term may be varied
artificially with a pitching rate differential collective pitch input
from an autopilot.
- $H_{\dot{x}}$ = rate of change of rotor horizontal force with translational velocity,
lbs.-sec./ft.
- $H_{\dot{\theta}}$ = rate of change of rotor horizontal force with fuselage pitching velocity,
lbs.-sec./ft.
- K = ratio of fuselage tilt to swash plate tilt, each relative to horizon.
This corresponds to an attitude cyclic pitch input from an autopilot.

4. Discussion of Simulation Theory

The theoretical problem of direct model simulation of a full scale helicopter is discussed in References 3 and 4. Therefore the subject will be discussed here only in a cursory manner sufficient to explain the tandem model design presented.

For the sake of simplicity it will be assumed that Reynolds Number and Mach Number effects are negligible¹ for the range considered, and that the traveling mass of the model is approximately equal to the lifted mass.² In general, however, these assumptions must be carefully examined and qualified.

When designing a model to simulate a full scale helicopter, the geometric parameters will be the same for the model if the full scale linear dimensions are reduced by a factor λ , where λ is defined as follows:

$$\lambda = \frac{\text{Given linear dimension of full scale helicopter}}{\text{Corresponding dimension of model}}$$

Dynamic simulation may be achieved if the model mass characteristics are obtained by using λ to the appropriate power and assuming that the density of the model construction material is the same as that for the full scale helicopter. The expressions for the model velocities and time scale may then be derived from the above factors by keeping in mind the fact that air density and gravitational acceleration are the same for the model and the full scale machine. The scale factors listed in Table I are based on this approach and were used in the HUP helicopter model design.

1. The primary effect of the small model Reynolds Number is an increase in the blade profile drag (Reference 4). This may be partially compensated for by using a thinner airfoil section on the model.
2. For the carriage and track facility considered in this case, the effective lifted mass may be artificially increased to compensate for the incremental traveling mass of the carriage by attaching a light fly wheel and pulley to the assembly which is lifted by the rotor. The required thrust coefficient may then be obtained with a down spring of approximately constant force.

5. Description of Model

As work on this project progressed it became apparent that direct simulation could not easily be obtained without eliminating the variable overlap and side-by-side features of the model. It was realized, however, that direct simulation of the HUP helicopter would in itself be a very important contribution. Therefore increased emphasis was placed on the simulation of the HUP helicopter at the expense of the other features of the model.

The model is designed to utilize the test facility described in Reference 1. This facility is composed of a horizontal track, a carriage and pylon, and a yoke; so arranged that the helicopter fuselage has complete freedom of motion in a vertical plane.

Preliminary drawings of the model are presented in Figures 1, 2, 3, and 4. Table II contains the parameters of the model and prototype. The model parameters were obtained by the method discussed in Section 4. A weight and balance estimate for the model may be found in Table III.

Power System (Figures 1 and 3)

The model is powered by an induction type 400 cycle 200 volt motor located at the approximate center of the fuselage. The motor is installed in the horizontal position so that the motor rotor comprises part of the shaft connecting the fore and aft rotor transmissions. The transmissions produce a 50 to 9 speed change and a 90° change in direction thru a bevel mesh and a spur mesh.

High power output at minimum material weight is obtained by utilizing the fuselage beams as mounting structure for the motor and by finning and baffling the motor windings to utilize the rotor downwash for cooling purposes. Calculations indicate that this installation will produce up to 1.5 hp without overheating.

Power will be supplied to the motor thru a "third rail system" and will be regulated with a motor-generator power source.

Control System (Figures 1 and 2)

The control system for this model presented a particular problem, since it was necessary to obtain close coordination between the fore and aft rotors for very small cyclic pitch variations.

Cyclic pitch on each rotor is obtained by tilting the control star (A), which is mounted on a ball and socket bearing at the center of the hub plate (B). The control star is attached to the blade pitch horns (C) as shown and rotates with the blades because of the drive (D) and the bearing at (E). Coordination of cyclic pitch between the fore and aft rotor is achieved by the cyclic pitch rods (F) and the links (G).

The proposed test procedure discussed in Section 7 required that a cyclic pitch input step function or sine wave be applied, and that the input be applied by an electric signal indicating that the model is in steady hovering flight. Either of these inputs may be obtained by using the hovering signal to engage the electric clutch and crank (H) to the gear train (J), which meshes with the rotor drive system. Rotation of crank (H) moves the cyclic pitch rods (G) axially and produces the control input. The gears in this train may be readily changed to obtain various drive frequencies, and micro switches are located so that the drive may be stopped after half a cycle.

Both the sine wave and an approximate step function may thus be obtained with the same basic drive mechanism; the difference being that for the step function the sine period is greatly reduced, and the drive is stopped after half a cycle.

Rotor Blade Construction (Figure 4)

As noted in Table II the required running blade weight for the model is .00708 lbs./in. Early design studies showed that this weight could not be met by conventional model construction methods if the blade chordwise center of gravity was also to be at the quarter chord. Accordingly, several less conventional, but extremely light, designs were laid out and the simplest design actually constructed during this phase of the program. Some practical insight was thereby obtained into what appears to be the most difficult model simulation design problem.

A detail drawing of the test model blade is shown in Figure 4, and a photograph of a blade blank and a completed blade (before lacquering) may be found in Figure 5. The calculated detail design characteristics of the blade (less lacquer and glue) are compared the final measured values below:

Test Blade Characteristics

	<u>Calculated</u>	<u>Measured</u>	
		doped	lacquered
Chordwise c.g., % chord.	22.2	24.3	25.3
Running weight, lbs./in.	.00647	.00625	.00671
Shear center, % chord	—	25.8	28.9
Torsional stiffness, GI_p , lbs.-in. ²	—	450	460
Bending stiffness, EI, lbs.-in. ²	1105	1280	1300

No calculation of the torsional stiffness or shear center was done, but a qualitative effort was made to keep the shear center near the quarter chord.

Since the blade was of wooden construction, warping was considered a primary problem, and considerable effort was made to seal out moisture. It was also necessary that the sealer not sink into the wood excessively and increase its weight, and that it be compatible with the glue used. Conventional model

airplane glue and dope were chosen because of their known characteristics in this respect.

Each piece of the blade was carefully dried and doped before construction of the blank. The blanks were then assembled as indicated in Figure 4 and thoroughly clamped. Alternate layers were laid cross grain to reduce warpage.

Previous experiments indicated that an adequate joint between the lead nose piece and the wood can be achieved provided the lead is absolutely clean.

The blade was next shaped by hand to a contour tolerance of $\pm .005$ inches, using sandpaper and metal templates. At this juncture the blade was painted with one coat of dope and the dimensional, inertial, and structural characteristics measured (see above list).

The blade was finished with four coats of blade lacquer. Any irregularities appearing after the first two coats were sanded down, and after the last coat the blade was dressed with crocus cloth, rubbing compound, and wax. The inertial and structural characteristics were then measured again (see above list).

It can be seen that this type of construction produces a blade that is light, properly balanced, and with desirable structural characteristics. It is recognized, however, that blade homogeneity and warpage may still present problems; although the present test blade has not warped excessively to date.

6. Theoretical Prediction of Results

In an effort to develop a satisfactory testing procedure the theoretical longitudinal characteristics of the HUP model were calculated near hovering flight, using a method essentially the same as that of Reference 6. The quantitative significance of the various aerodynamic parameters was investigated to determine which ones are of major importance. The effects of a simple autopilot were also considered by calculating the influence on the model motion of variations in the aerodynamic parameters which can readily be changed artificially.

Because of the preliminary nature of this investigation the fuselage, pitch oscillation and damping, and the control response to a sudden control displacement were calculated for a range sufficiently large to include the probable values of the parameters.

It was found that the rate of change of horizontal rotor force with translational velocity, H_x , is a very significant parameter for the tandem helicopters just as it is for single-rotor machines. The rate of change of horizontal rotor force with pitching velocity, H_q , however, contributes negligible pitch damping compared to the pitch damping, $\frac{1^2 Z}{2}$, due to the fore and aft rotor rate of change of thrust with vertical velocity. This differs from the case of the single-rotor helicopter where H_q is the significant damping term.

The effects of H_x and $\frac{1^2 Z}{2}$ on the period, damping, and control response are plotted in Figures 6, 7, and 8. It can be seen in Figures 6 and 7 that the period and damping are affected by both $\frac{1^2 Z}{2}$ and H_x to a considerable extent. While values of $\frac{1^2 Z}{2}$ below 6.25 cause considerable divergence; i.e., positive damping exponents, larger values only cause moderate convergence. As $\frac{1^2 Z}{2}$ increases the effect of H_x rapidly diminishes.

The range of values for $\frac{V^2}{2}$ includes the value 8.30, which is based on the assumption that the rotor induced velocity is dependent only on the steady hovering conditions; and the value 2.87, which is based on the assumption that the rotor induced velocity depends on the hovering conditions and the instantaneous vertical velocity of each rotor. Qualitative flight observations on the full scale helicopter indicate that the correct value approaches 8.30.

As pointed out in Reference 1, the accurate prediction of the collective pitch angle has a great influence on H_x . The three values of H_x used were therefore determined in the following manner. The collective pitch angle (9.4 degrees) was determined using momentum theory and tip loss, assuming a constant induced velocity distribution over the disc. Values of 7.0 degrees and 11.0 degrees were included to provide sufficient range for inaccuracies in the collective pitch theory. The values of H_x corresponding to these collective pitch angles were then used to calculate the model dynamic characteristics.

Longitudinal control on the full scale helicopter is composed of a combination of cyclic pitch and differential collective pitch. This type of system will therefore be used in work for comparison with full scale data. It was found, however, that differential collective pitch is an excessively powerful control. Displacement increments that are large enough to be accurately measured produce fuselage responses which are too large for use in evaluating a linearized theory. Pure cyclic pitch inputs were therefore used to obtain the analytical responses plotted in Figures 8 and 10. It can be seen in Figure 8 that again variations in H_x and $\frac{V^2}{2}$ have considerable effect on the motion.

An attempt to improve the handling qualities of the helicopter with an autopilot was made by considering the influence of artificial variations in the aerodynamic parameters.

The effects of cyclic pitch proportional to translational velocity, pitching velocity, and fuselage pitch angle were investigated, and differential collective pitch proportional to fuselage pitching velocity was also considered.

As mentioned previously the major portion of pitch damping is due to $\frac{12\pi}{2}$, not H_z , so cyclic pitch proportional to pitching velocity produces little increase in stability. Since variations in H_z are equivalent to cyclic pitch proportional to translational velocity, it can be seen from Figure 6 that here again little increase in stability is obtained.

The changes in the oscillation damping exponent when cyclic pitch proportional to fuselage pitch angle and differential collective pitch proportional to fuselage pitching velocity are applied indicated that stability might be obtained using these two control inputs. From Figure 9 it may be seen that the optimum value for $\frac{12\pi}{2}$ is approximately 3.0 for the range of variables considered. It was therefore assumed that the autopilot applied differential collective pitch proportional to pitching rate which would produce this value.

A translational velocity response to a sudden 1.0 degree cyclic pitch application was then calculated for two values of pitch attitude input; one for which the inclination of the swash plate was 95% of the fuselage tilt relative to the horizon ($K = .95$), and one for which the swash plate inclination was 90% of the fuselage tilt relative to the horizon ($K = .90$).

These two responses are compared to the response of the pure helicopter ($K = 1.0$) in Figure 10. The translational velocity response was calculated rather than the attitude response because, as the helicopter is stabilized, it is important that there be no reduction in the pilot's ability to maneuver the machine. Both autopilot inputs increase the initial response without reducing the trim velocity, and the response for the 90% cyclic input may be

considered extremely satisfactory in all respects.

In the process of the above investigation a coupling action of considerable magnitude was discovered between longitudinal and directional modes of motion. As previously mentioned, when the helicopter oscillates in pitch, the rotors produce a differential thrust damping moment due to the local vertical velocities at each rotor. These differential thrusts produce differential torques on the rotor shafts because of the changes in induced power for each rotor. Since the rotors turn in opposite directions, the torques are additive and are of sufficient magnitude to produce yaw angles comparable to the pitch angles.

The power required to hover out of ground effect was calculated using a method outlined in Reference 5 and is plotted in Figure 11. This curve was used to determine the motor size required for the model.

7. Proposed Instrumentation and Test Procedure

The period of oscillation, oscillation damping exponent, and pitching and translational response to a sudden control disturbance will be obtained for a range of rotor speeds and lifted weights within the performance limitations of the model.

Experience with a previous model (Reference 1) has shown that, in obtaining repeatable data of the above type, it is necessary that each run be started from an absolute dead hovering condition and that translational friction and pitching friction be very consistent in nature and an absolute minimum in magnitude. Therefore, in order to reduce friction to the required minimum, the trailing control and power cables described in Reference 1 will not be used here. Rotor speed and fuselage pitching angle signals will be transmitted on the third rail power supply system, and the translational motion data will be obtained with contact switches appropriately located along the track as was done in Reference 1. The collective pitch will be ground adjustable and thrust control will be obtained by regulation of rotor speed through the motor generator power source. Cyclic pitch input is of the escapement type (see Section 5), and the amplitude is also measured with the rotor inoperative. In cases where a sinusoidal cyclic pitch input is required, the period of the input can be obtained knowing the rotor speed and the cyclic pitch drive gear ratio.

Flight procedure will be as follows: The collective pitch will be set at the value required for hovering flight at the test rotor speed. The model will then be placed on a take-off stand which will support it at the test attitude and will swing out of the way after take-off. (The contact points between the model and the stand will be designed so that at the moment the model rises from the stand the cyclic pitch input is applied). Next the rotor will be

brought up to speed so that the model gently lifts off the stand, and the cyclic pitch disturbance is introduced. The model will be allowed to fly freely until the required data has been obtained or a dangerous attitude has been reached. The flight will be terminated by cutting the power and allowing the model to settle on its supporting carriage. Model motion stops will be provided as a precaution against excessive model attitudes, and all recorded data will be obtained with an oscillograph.

The theoretical analysis of section 6 indicates that, depending on the value of $\frac{1^2 \eta}{2}$, either a divergent or a convergent oscillation may be obtained. In the event that the motion is divergent no cyclic input will be necessary at take-off, since the motion will build up from any infinitely small disturbance. If the motion is convergent a sinusoidal cor rol input will be applied as discussed above, and the period and damping will be obtained with frequency response techniques.

Since $\frac{1^2 \eta}{2}$ is such an important parameter, this term will also be determined independently. The translational motion of the model will be restrained and each rotor thrust time history will be measured while the model is forced to oscillate sinusoidally in pitch.

At the completion of the above tests, the model control system will be modified to simulate the full scale system i.e., differential collective pitch will be added, and the control response test repeated. This model data will then be available for comparison purposes when full scale hovering stability and control data becomes available on an HUP helicopter.

8. Concluding Remarks

A tandem rotor helicopter model has been designed to investigate experimentally the longitudinal hovering stability and control characteristics of this helicopter configuration. The parameters of the model have been chosen so that direct dynamic simulation of the Piasecki HUP helicopter should be obtained.

The simulation theory requires an extremely light blade design. Therefore, a test section of the model blade has been actually constructed to prove the feasibility of a typical design.

The results of a theoretical dynamic analysis have been presented to gain some insight into the handling qualities of the model. This information has been used to determine an adequate test and instrumentation procedure for the model and to investigate means for improving the hovering qualities of this type of helicopter.

The analysis indicates that excellent longitudinal hovering characteristics may be obtained by introducing differential collective pitch proportional to pitching rate and cyclic pitch proportional to pitch angle. The analysis also indicates that for the pure helicopter, differential induced torque effects produce considerable coupling between the longitudinal and directional modes of motion.

9. References

1. Gray, McCaskill, Gebhard, and Goland, "Model Study of Helicopter Dynamic Stability and Control, Phase II, Comparison of Theoretical and Experimental Results Near Hovering Flight," Princeton University Aero. Eng. Lab. Report No. 230, May, 1953.
2. Gray, R., "Model Study of Helicopter Dynamic Stability and Control, Model Rotor Test Stand," Princeton University Aero. Eng. Lab. Report No. 250, November, 1953.
3. Brooks, George W., "The Application of Models to Helicopter Vibration and Flutter Research," Proceedings of the Ninth Annual Forum, American Helicopter Society, May, 1953.
4. Goland, L., "On the Design of Models for Helicopter Research and Development," Princeton University Aero. Eng. Lab. Report No. 240, October, 1953.
5. Nikolsky, A. A., "Helicopter Analysis," John Wiley and Sons, Inc., 1951.
6. Gebhard, J. G., "Tandem Helicopter Longitudinal Stability and Control," Princeton University Aero. Eng. Lab. Report No. 233, June, 1953.

Table I. Scale Factors for Dynamic Simulation

λ = Linear dimension of full scale helicopter
Corresponding dimension of model

Parameter	Factor
Linear dimensions	λ^{-1}
Area	λ^{-2}
Volume, Mass, Force	λ^{-3}
Moments	λ^{-4}
Mass moments of inertia	λ^{-5}
Linear velocity, time	$\lambda^{-\frac{1}{2}}$
Linear acceleration	λ^0
Angular velocity	$\lambda^{\frac{1}{2}}$
Angular acceleration	λ
Power	$\lambda^{\frac{3}{2}}$

Note: Other parameters may be derived based on the above expressions.

For example, modulus of elasticity is usually defined in pounds/inch².

$$\frac{\lambda^{-3}}{\lambda^{-2}} = \lambda^{-1}$$

λ^{-1} is therefore the scale factor for modulus of elasticity.

Table II. Prototype and Model Parameters ($\lambda = 8.86$)

	Prototype ¹	Model
Gross weight, lbs.	5700	28.5
No. of blades	3	3
Blade radius, ft.	17.58	3
Blade chord (constant), in.	13	2.22
Rotor angular velocity, rad./sec.	30.6	73.8
Blade airfoil section (N.A.C.A.)	63015	0012 ²
Blade twist, radians	unknown	0 ³
Slope of lift curve, a	5.75	5.75
R.N. at 3/4 radius	2.8×10^6	1.95×10^5
Spanwise flapping hinge offset, in.	2	.341
Chordwise feathering axis offset, in.	1 fwd.	.170 fwd.
Spanwise position of drag hinge, in.	15	— ⁴
Blade flapping moment of inertia, slug ft.	163.94	.0239 ⁵
Blade static moment, slug ft.	15.06	.0128
Pitching moment of inertia, slug ft. ²	10714	1.55
Distance between rotors, in.	263	44.8
Distance from c.g. to fwd. rotor, in.	131.5	22.4
Height of fwd. rotor above c.g., in.	64.1	10.94
Height of rear rotor above c.g., in.	93.1	15.9
Power, hp.	350	1.15

1. The prototype was a Piasecki HUP-2 with metal blades.
2. See Section 4 for discussion of change in blade section.
3. For this study the effects of blade twist were assumed to be negligible.
4. For the hovering flight range the drag hinges were not considered necessary.
5. A design blade running weight of .00703 lbs./in. was determined from this value.

Table III. Model Weight and Balance

Moments, Horizontal Direction: (z = vertical distance from mounting point)

	<u>Wt. (lbs.)</u>	<u>z (in.)</u>	<u>Wz</u>
Fwd. Rotor head	1.5	10.8	16.2
Fwd. Rotor blades	1.1	10.8	11.9
Rear Rotor head	1.5	14.05	21.1
Rear Rotor blades	1.1	14.05	15.5
Fwd. Trans.	2.5	-2.2	-5.5
Rear Trans.	2.5	-2.2	-5.5
Motor	4.81	-3	-14.4
Other	<u>13.5</u>	<u>-2.91</u>	<u>-39.3</u>
	28.5		0

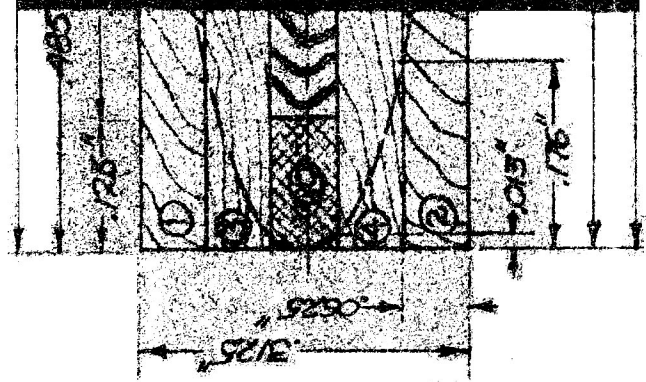
Moments, Vertical Direction: (x = horizontal distance from mounting point)

	<u>Wt. (lbs.)</u>	<u>x (in.)</u>	<u>Wx</u>
Fwd. Rotor head	1.5	22.4	33.6
Fwd. Rotor blades	1.1	22.4	24.6
Rear Rotor head	1.5	-22.4	-33.6
Rear Rotor blades	1.1	-22.4	-24.6
Fwd. Trans.	2.5	21.8	54.5
Rear Trans.	2.5	-21.8	-54.5
Motor	4.81	-0.5	-2.4
Other	<u>13.5</u>	<u>+0.18</u>	<u>2.4</u>
	28.5		0

NOTE: SECTIONS ③, ④, ⑥, & ⑦ SHOWN CUT WITH GRAIN. ALL OTHER SECTIONS SHOWN CUT CROSS GRAIN



SECTION
(FULL SCALE)

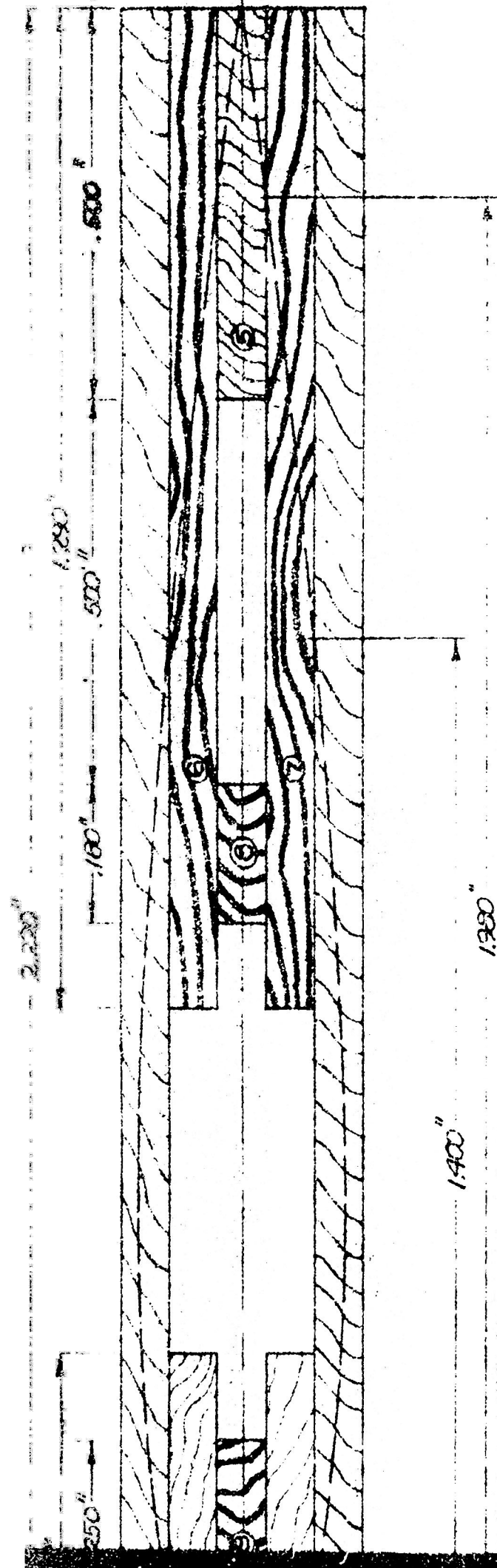


20"

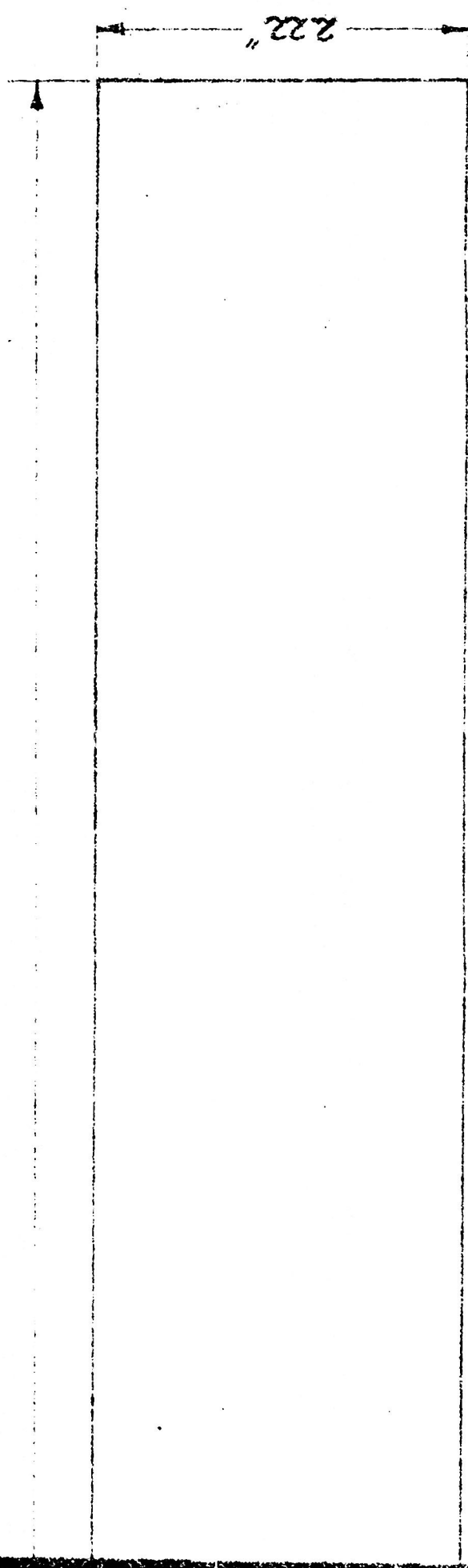
1. NAME(S)
 2. AGE
 3. SEX
 4. RACE
 5. RELIGION
 6. EDUCATION
 7. PROFESSION
 8. RESIDENCE
 9. DATE
 10. SIGNATURE
 11. ADDRESS
 12. CITY
 13. STATE
 14. ZIP
 15. TELEPHONE
 16. TELETYPE
 17. TELEFAX
 18. EMAIL
 19. WEB
 20. MOBILE
 21. HOME
 22. WORK
 23. CELL
 24. PAGER
 25. TELEVISION
 26. RADIO
 27. VIDEO
 28. CD
 29. DVD
 30. MP3
 31. MP4
 32. MP5
 33. MP6
 34. MP7
 35. MP8
 36. MP9
 37. MP10
 38. MP11
 39. MP12
 40. MP13
 41. MP14
 42. MP15
 43. MP16
 44. MP17
 45. MP18
 46. MP19
 47. MP20
 48. MP21
 49. MP22
 50. MP23
 51. MP24
 52. MP25
 53. MP26
 54. MP27
 55. MP28
 56. MP29
 57. MP30
 58. MP31
 59. MP32
 60. MP33
 61. MP34
 62. MP35
 63. MP36
 64. MP37
 65. MP38
 66. MP39
 67. MP40
 68. MP41
 69. MP42
 70. MP43
 71. MP44
 72. MP45
 73. MP46
 74. MP47
 75. MP48
 76. MP49
 77. MP50
 78. MP51
 79. MP52
 80. MP53
 81. MP54
 82. MP55
 83. MP56
 84. MP57
 85. MP58
 86. MP59
 87. MP60
 88. MP61
 89. MP62
 90. MP63
 91. MP64
 92. MP65
 93. MP66
 94. MP67
 95. MP68
 96. MP69
 97. MP70
 98. MP71
 99. MP72
 100. MP73
 101. MP74
 102. MP75
 103. MP76
 104. MP77
 105. MP78
 106. MP79
 107. MP80
 108. MP81
 109. MP82
 110. MP83
 111. MP84
 112. MP85
 113. MP86
 114. MP87
 115. MP88
 116. MP89
 117. MP90
 118. MP91
 119. MP92
 120. MP93
 121. MP94
 122. MP95
 123. MP96
 124. MP97
 125. MP98
 126. MP99
 127. MP100
 128. MP101
 129. MP102
 130. MP103
 131. MP104
 132. MP105
 133. MP106
 134. MP107
 135. MP108
 136. MP109
 137. MP110
 138. MP111
 139. MP112
 140. MP113
 141. MP114
 142. MP115
 143. MP116
 144. MP117
 145. MP118
 146. MP119
 147. MP120
 148. MP121
 149. MP122
 150. MP123
 151. MP124
 152. MP125
 153. MP126
 154. MP127
 155. MP128
 156. MP129
 157. MP130
 158. MP131
 159. MP132
 160. MP133
 161. MP134
 162. MP135
 163. MP136
 164. MP137
 165. MP138
 166. MP139
 167. MP140
 168. MP141
 169. MP142
 170. MP143
 171. MP144
 172. MP145
 173. MP146
 174. MP147
 175. MP148
 176. MP149
 177. MP150
 178. MP151
 179. MP152
 180. MP153
 181. MP154
 182. MP155
 183. MP156
 184. MP157
 185. MP158
 186. MP159
 187. MP160
 188. MP161
 189. MP162
 190. MP163
 191. MP164
 192. MP165
 193. MP166
 194. MP167
 195. MP168
 196. MP169
 197. MP170
 198. MP171
 199. MP172
 200. MP173
 201. MP174
 202. MP175
 203. MP176
 204. MP177
 205. MP178
 206. MP179
 207. MP180
 208. MP181
 209. MP182
 210. MP183
 211. MP184
 212. MP185
 213. MP186
 214. MP187
 215. MP188
 216. MP189
 217. MP190
 218. MP191
 219. MP192
 220. MP193
 221. MP194
 222. MP195
 223. MP196
 224. MP197
 225. MP198
 226. MP199
 227. MP200
 228. MP201
 229. MP202
 230. MP203

QUERIES

20 x .5625 x 2.200
 20 x .0625 x .455
 20 x .0325 x .300
 20 x .0515 x 1.200
 20 x .0625 x .180
 20 x .0615 x .250
 20 x .0525 x .125



SECTION SHOWING STRUCTURAL DETAIL
(SCALE - 5 INCHES = 1 INCH)



ALL INFORMATION CONTAINED HEREIN IS UNCLASSIFIED

[Faint handwritten signature]

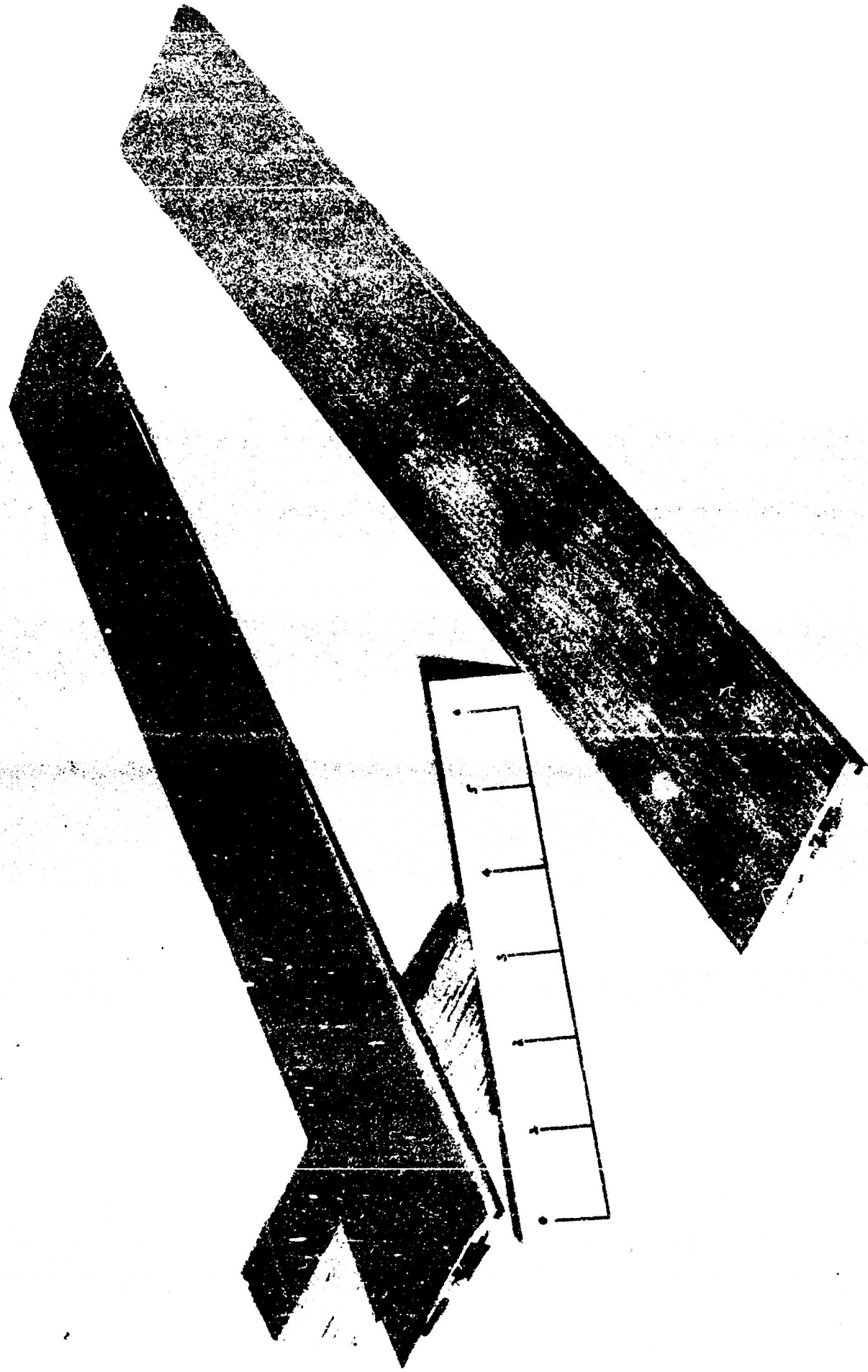


FIGURE 5.

COMPLETED HUP MODEL HELICOPTER TEST BLADE AND BLADE BLANK

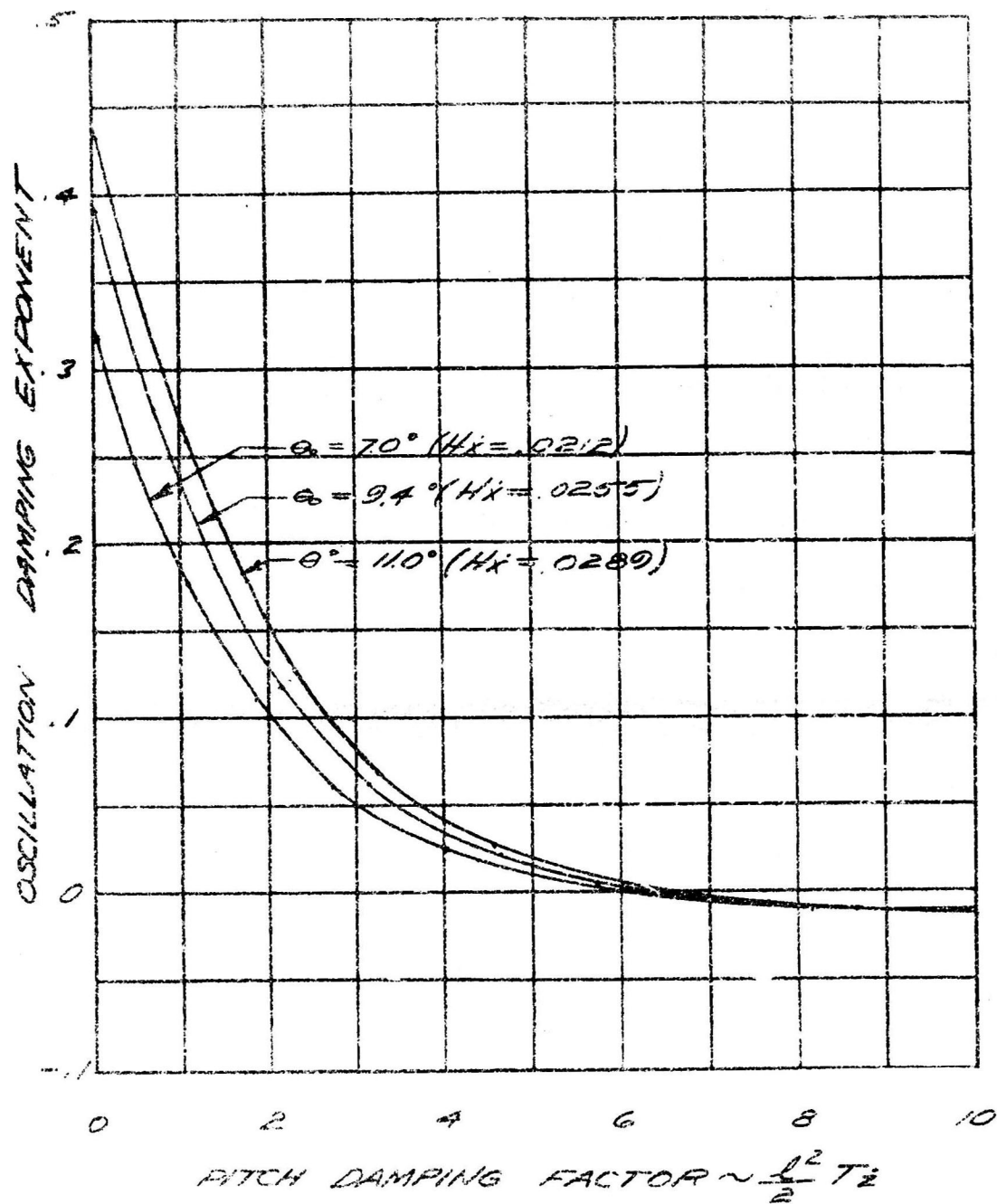


Fig. 6 Effect of $\frac{1}{2} T_2$ and H_x on Fuselage Oscillation Damping Exponent.

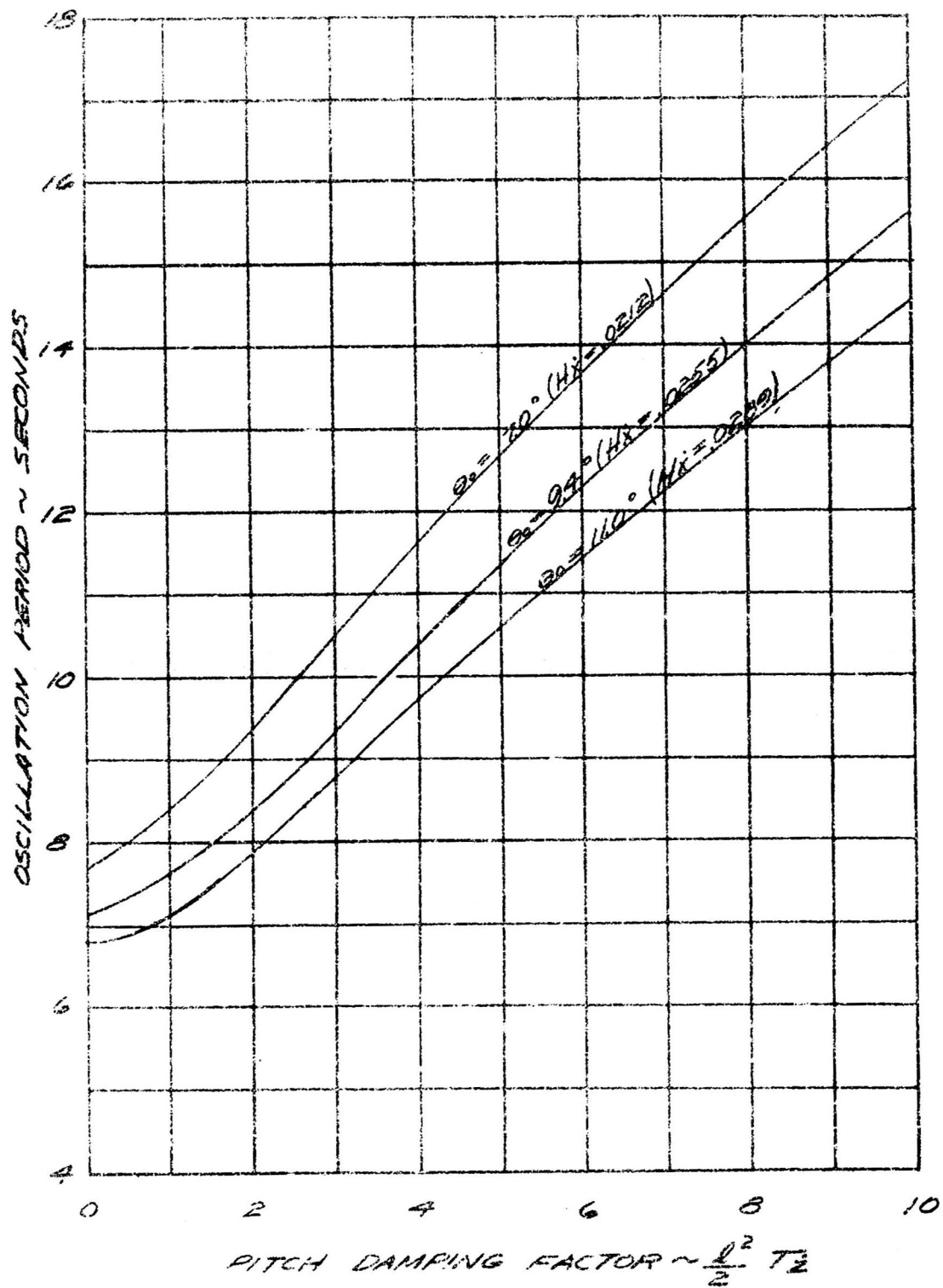


Fig. 7 Effect of $\frac{1}{2} T_2^2$ and H_x on Fuselage Oscillation Period.

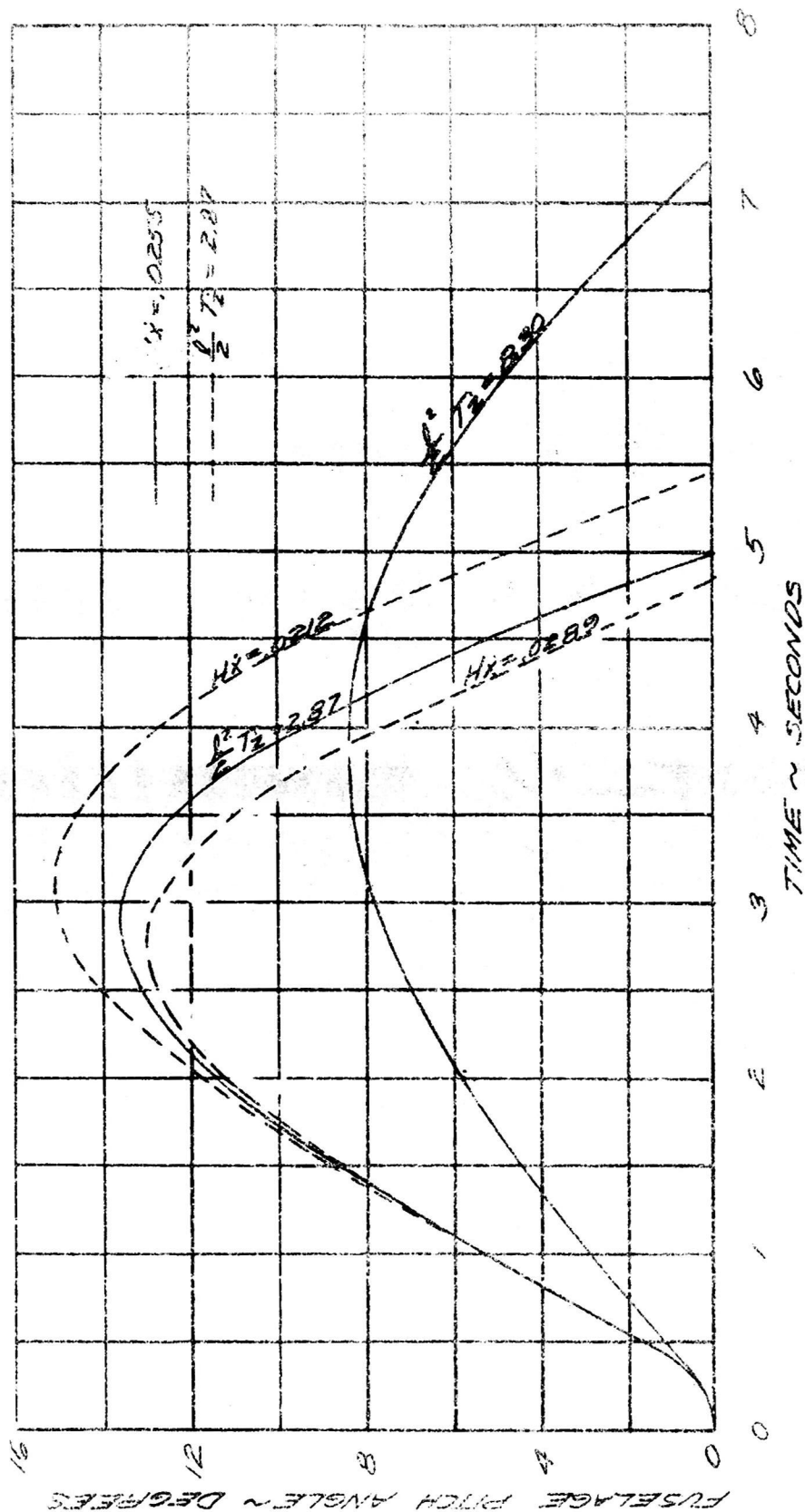


FIG. 8 Effect of $\frac{1}{2}T_2$ and H_x on Fuselage Pitch Response to a Sudden 1.0 Degree Cyclic Pitch Displacement.

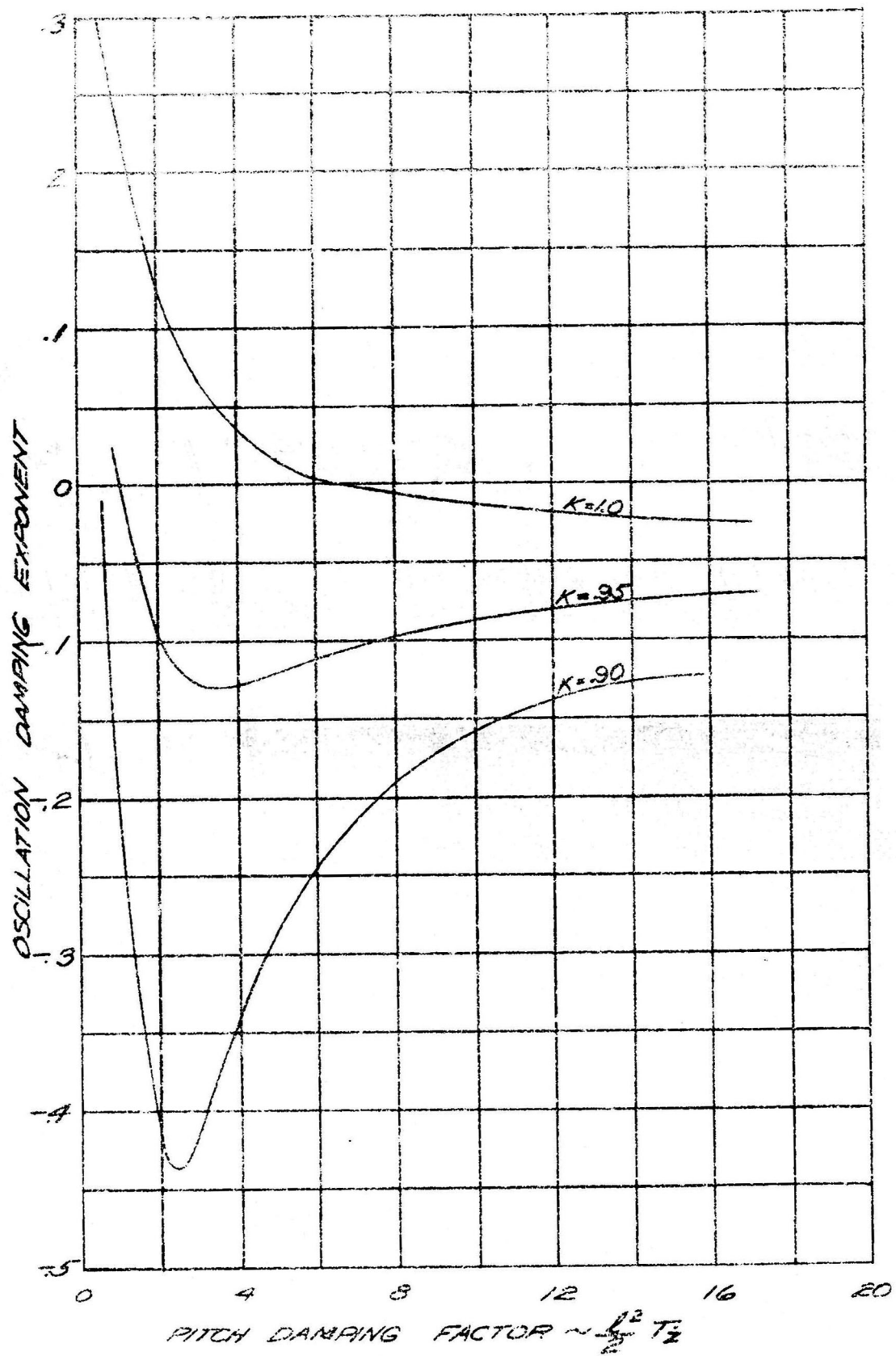


Fig. 9 Effect of $\frac{1}{2} T_z^2$ and K on Fuselage Oscillation Damping Exponent.

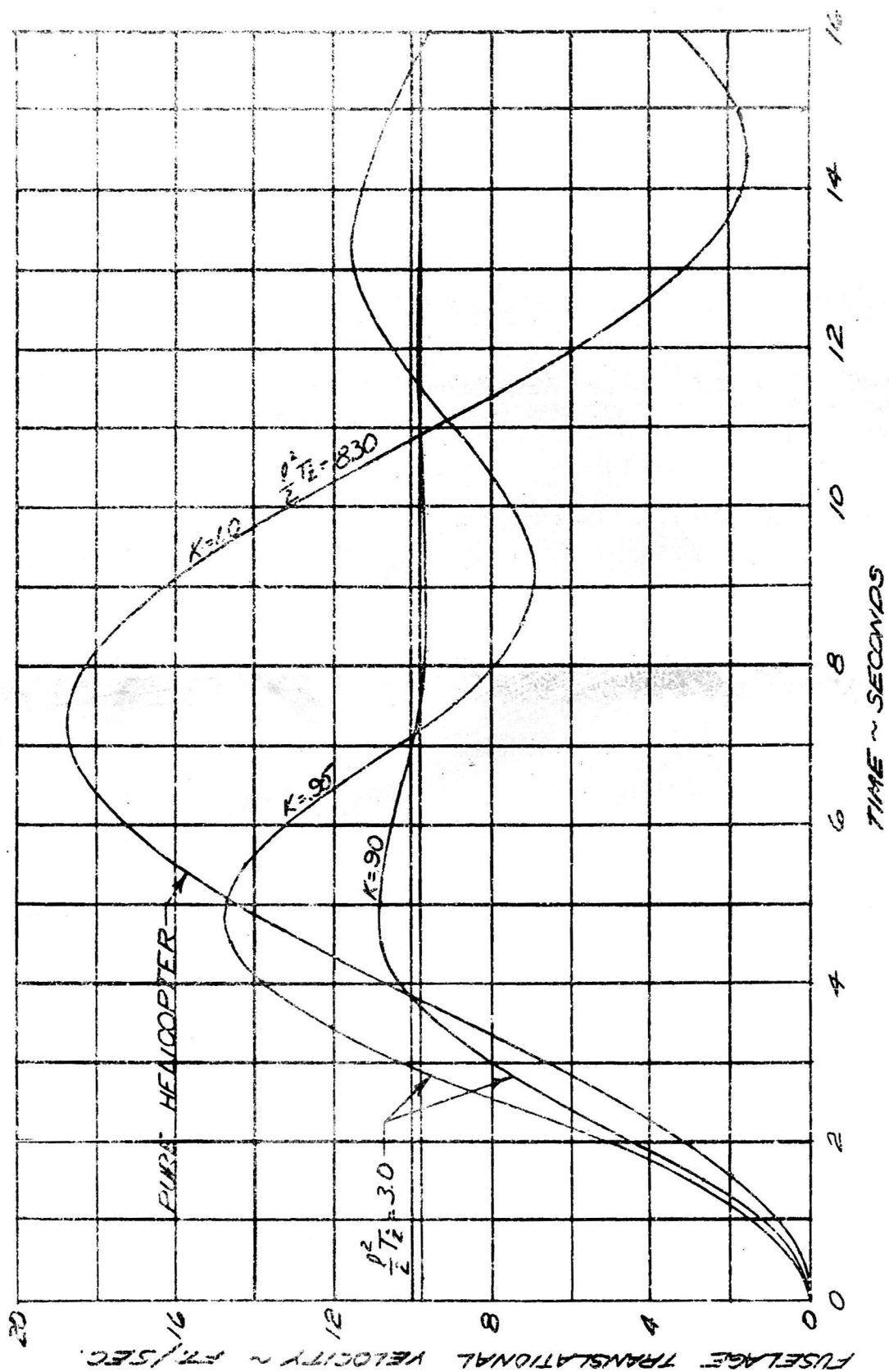


Fig. 10 Effect of $\frac{p^2}{T^2}$ and K on Fuselage Translational Response to a Sudden 1.0 Degree Cyclic Pitch Displacement.

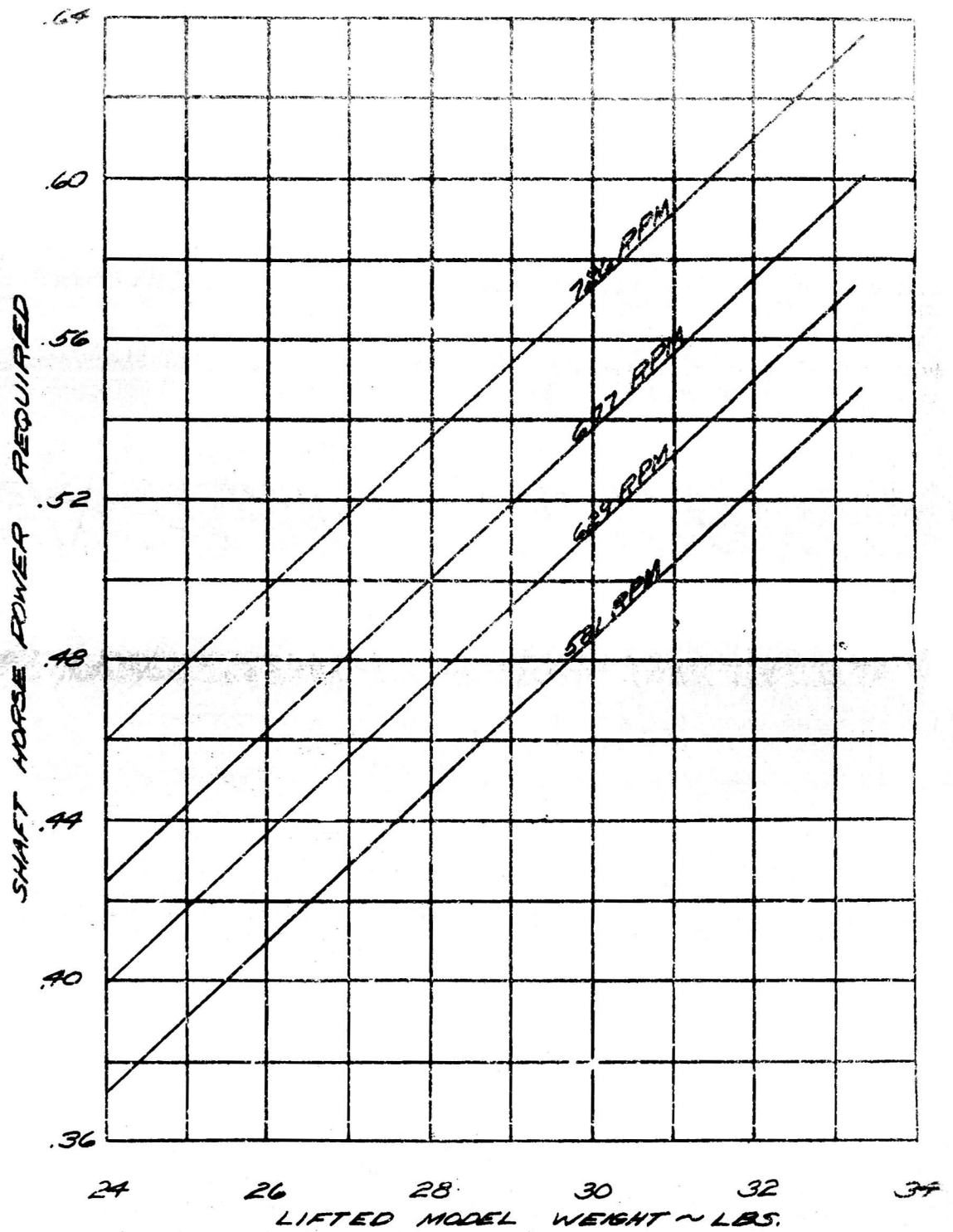


Fig. 11 Model Power Required vs. Lifted Weight at Various Rotor Speeds.